ACS APPLIED MATERIALS & INTERFACES

Letter

www.acsami.org

Synergistically Enhanced Stability of Highly Flexible Silver Nanowire/Carbon Nanotube Hybrid Transparent Electrodes by Plasmonic Welding

Jongsoo Lee,‡ Ju Yeon Woo,‡ Ju Tae Kim, Byung Yang Lee, and Chang-Soo Han*

School of Mechanical Engineering, Korea University, Anam-Dong, Seongbuk-Gu, Seoul 136713, Korea

Supporting Information

ABSTRACT: Here, we report highly transparent and flexible AgNW/SWCNT hybrid networks on PET substrates combined with plasmonic welding for securing ultrahigh stability in mechanical and electrical properties under severe bending. Plasmonic welding produces local heating and welding at the junction of AgNWs and leads strong adhesion between AgNW and SWCNT as well as between hybrid structure and substrate. The initial sheet resistance of plasmon treated AgNW/SWCNT hybrid film was 26 Ω sq^{-1}, with >90% optical transmittance over the wavelength range 400–2700 nm. Following 200 cycles of convex/concave bending with a bending radius of 5 mm, the sheet resistance changed from 26 to 29 Ω sq^{-1}. This hybrid structure combined with the plasmonic welding process provided excellent stability, low resistance, and high transparency, and is suitable for highly flexible electronics applications, including touch panels, solar cells, and OLEDs.

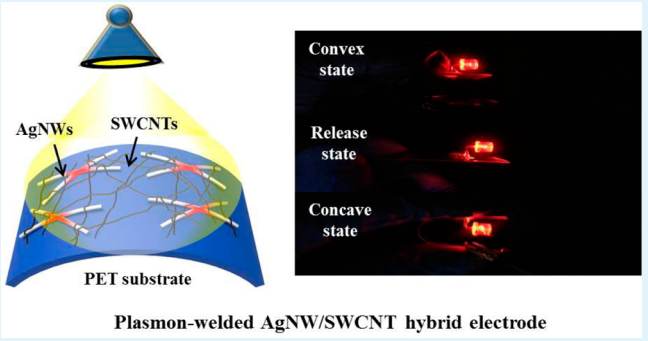

Plasmon-welded AgNW/SWCNT hybrid electrode

KEYWORDS: *silver nanowires, carbon nanotubes, plasmonic welding, transparent electrodes, flexible electronics*

Transparent conductive electrodes (TCEs) are regarded as a core component of various thin-film optoelectronic devices, including flat-panel displays, touch screens, solar cells, and organic light-emitting diodes (OLEDs).[1−4] To date, indium tin oxide (ITO) has been the most common transparent conducting material for these applications. Recently, incorporating mechanical flexibility into TCEs has received significant interest as a key technology for next-generation optoelectronic devices.[5−8] ITO is a brittle ceramic and requires careful deposition in vacuum; this, combined with growing material costs, makes ITO electrodes unsuitable for use in highly flexible or bendable electronic devices.[9,10] Therefore, several potential candidate materials, including conducting polymers,[11,12] carbon nanotubes (CNTs),[13−15] graphene,[16−18] and metallic nanowires,[19−21] have been investigated as alternatives to ITO. However, these materials have not yet been shown to be suitable replacements for ITO because of the poor conductivity and lack of stability of the conducting polymers,[9,22] relatively high sheet resistance at high transmittance (100 to 500 Ω sq^{-1} with a transparency of 80–95% at 550 nm), environmental issue of the chemical processes, and high cost of the carbon-based nanomaterials.[7,23]

Silver nanowires (AgNWs) have attracted much recent research interest as an alternative to ITO due to their straightforward fabrication, high conductivity, and mechanical ductility, as well as high corrosion stability.[24−27] However, in order to effectively integrate AgNW networks into flexible or bendable electronics, the following issues must be addressed: (1) the weak bonding between nanowires, resulting in degradation of mechanical and electrical stability; (2) the gaps between the AgNWs, which cause parasitic lateral current flow; (3) the mechanical fracture under large bending or stretching due to the rigidity of the nanowires; (4) the poor adhesion between the nanowires and plastic substrates; and (5) the poor infrared (IR) transmittance.[28] A particular challenge for AgNW transparent electrodes on plastic substrates is to prevent the AgNWs from being peeled off and broken at the junctions between nanowires under repeated strain. Although significant progress has been made in AgNW transparent electrodes using advanced processing methods, including mechanical pressing,[29,30] thermal annealing,[24,27,31,32] plasmonic welding,[2,33] incorporating additional conducting materials,[7,23,34] and layer transfer methods,[19,35] most reported methods resolve only some of the above issues, and the application of these methods is limited to certain types of device structures. Therefore, it is necessary to develop new processing methods and material structure for high-performance stable flexible TCEs.

Here, we describe a novel approach using AgNW/single-walled carbon nanotube (SWCNT) hybrid structures combined with a low-temperature plasmonic welding process. We

Received: April 30, 2014
Accepted: June 27, 2014
Published: June 27, 2014

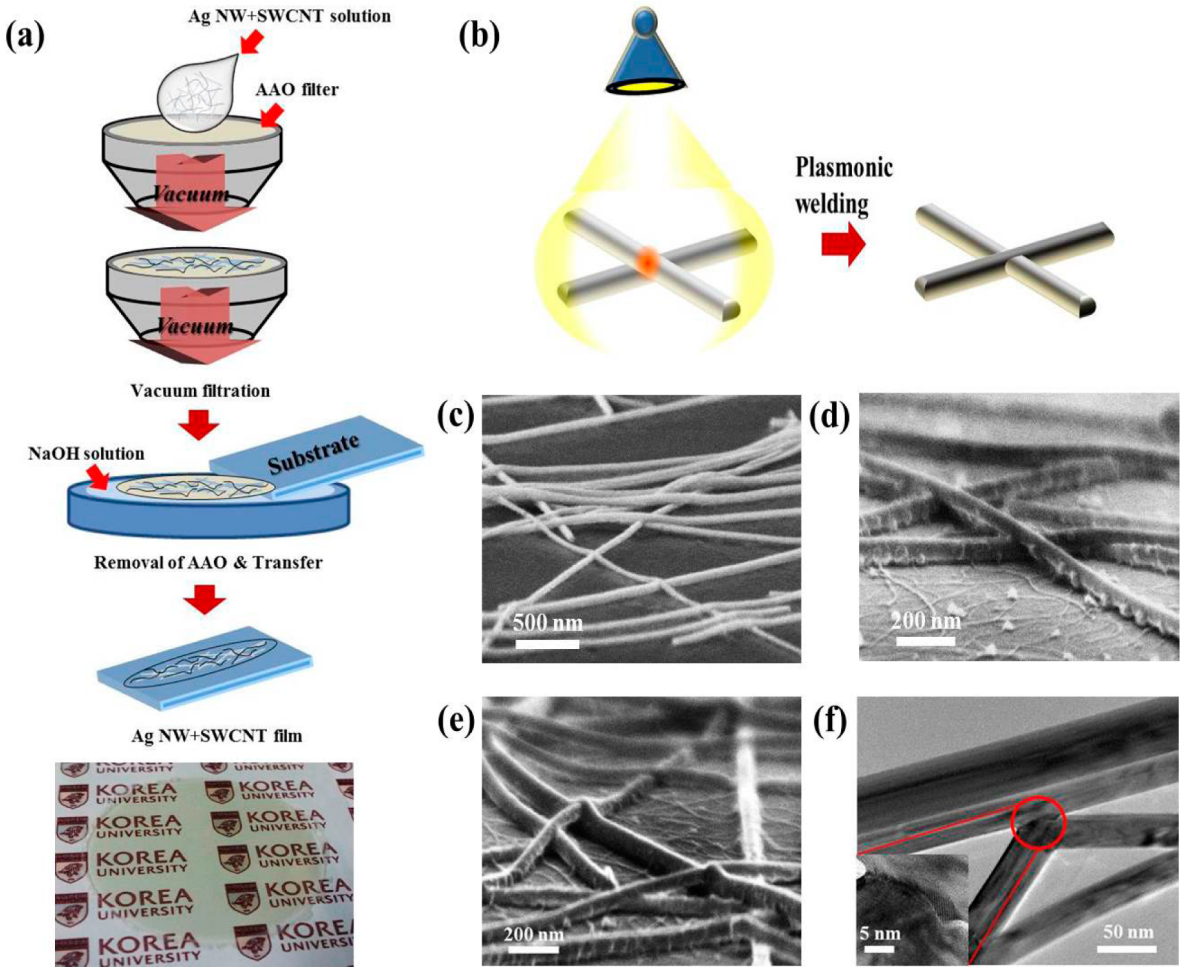

Figure 1. (a) Schematic diagram showing the AgNW/SWCNT hybrid film fabrication procedure. Bottom inset picture shows photograph of a highly transparent AgNW/SWCNT hybrid film on a PET substrate. (b) Schematic diagram illustrating the AgNW junction plasmonic welding process. Tilted cross-sectional SEM images of (c) AgNW networks, (d) AgNW/SWCNT hybrid structures, and (e) plasmonic-welded AgNW/SWCNT networks on a silicon wafer. (f) TEM images of AgNW junctions after optical plasmonic welding. The inset is a higher-magnification TEM image showing the plasmon-welded spot between AgNWs.

demonstrate that SWCNTs form flexible conducting networks with the AgNWs, which helps to efficiently collect free charges at the gaps in the AgNW network, as well as to enhance the stability of the conductivity by creating continuous conduction pathways. SWCNTs can aid in providing connections between AgNWs and the substrate, greatly enhancing the flexibility. In addition, we demonstrate films that are highly transparent in the infrared region (700−2700 nm) using AgNW/SWCNT hybrid electrodes. We found that plasmonic welding leads to strong bonding at the AgNW junctions, giving improved electrical and mechanical stability. As a result, plasmon-welded AgNW/SWCNT hybrid electrodes maintain excellent mechanical flexibility with high transmittance (92.3%), as well as low sheet resistance (29 Ω sq^{-1}) even under severe concave and convex cyclic deformation. The combination of plasmonic welding and hybrid AgNW/SWCNT materials produce indeed unexpected and extraordinary result in mechanical and electrical stability. For this, we achieve synergistic combination based on experimental data not simple combination.[2,23] In addition, we successfully fabricated a highly flexible light-emitting diode (LED) integrated circuit using our AgNW/SWCNT hybrid electrodes.

Figure 1a shows a schematic diagram of the fabrication process of the AgNW/SWCNT hybrid films. In the experiments here, AgNW/SWCNT hybrid films were prepared by filtration method to achieve good uniformity, to remove the surfactant easily and to avoid agglomeration onto flexible polymer substrate. In order to develop mass producible coating method, the effective removal method of surfactants should be developed. The dimensions of the AgNWs play an important role in the percolated network of conductive metal nanowires for flexible TCEs (see Figure S1 in the Supporting Information). Various volumes of the prepared AgNW and SWCNT dispersions were collected using a membrane filter with a pore size of 0.2 μm, which has been widely used in TCE fabrication.[36] Following vacuum filtration, an NaOH solution was used to remove the membrane. The floating AgNW/SWCNT films were transferred to the PET substrates, forming a flexible conducting layer. Bottom inset picture shows a digital photograph of the fabricated AgNW/SWCNT hybrid film on the poly(ethylene terephthalate) (PET) substrate, showing no structural damage. The film is highly transparent, which can be seen from the fact that the letters in the background are clearly visible through the film.

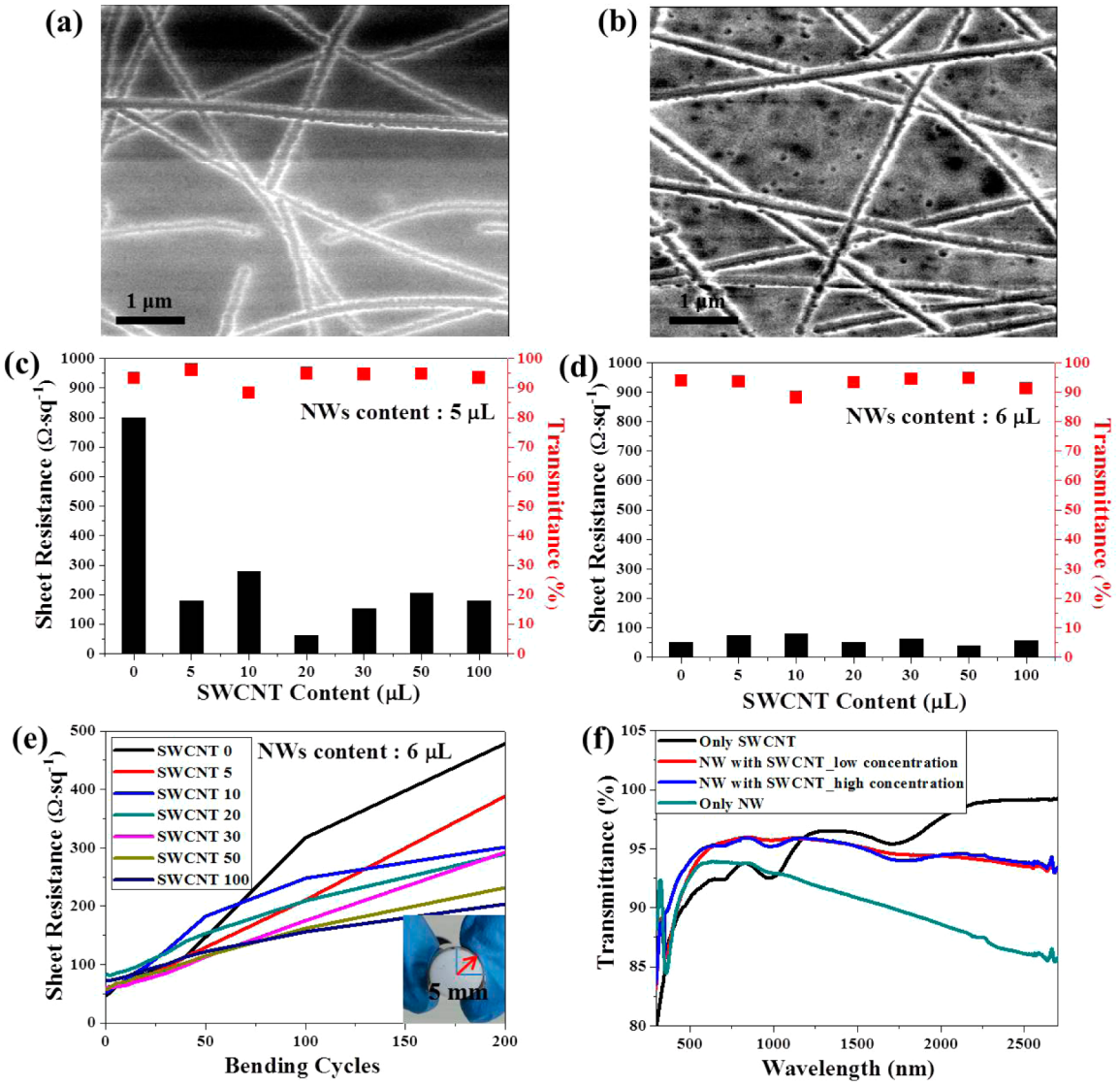

Figure 2. EFM images of (a) AgNW networks, and (b) AgNW/SWCNT hybrid structures on a PET substrate. Sheet resistance and transmittance as a function of CNT content for (c) 5 μL of AgNW solutions, and (d) 6 μL of AgNW solutions. Optical transmittance at the wavelength of 550 nm was measured. (e) Sheet resistance as a function of convex bending cycle for different CNT content before plasmonic welding. Inset shows the mechanical bend test conditions. (f) The optical transmittance spectra of a SWCNT film, an AgNW film, and AgNW/SWCNT hybrid films on PET substrate.

To fabricate highly flexible AgNW/SWCNT hybrid transparent electrodes with low sheet resistance, the AgNWs in the network should be strongly connected to each other. Recently, it was reported that a plasmonic nanowelding technique can improve the electrical properties through localized melting and fusion between the AgNW nanowires without significantly affecting the surrounding materials.[2,33] Figure 1b shows a schematic diagram of the plasmonic welding procedure, which uses a broadband tungsten/halogen lamp. At the AgNW junctions, there are nanometer-scale small gaps between the upper and lower AgNWs; these gaps enable extreme local heating due to the optical radiation coupling with plasmonic modes.[37] This local plasmonic welding facilitates good electrical conductivity and mechanical stability of the AgNW/SWCNT hybrid films under large mechanical strain. Figures 1c–e show tilted cross-sectional scanning electron microscopy (SEM) images of AgNW-only networks, the AgNW/SWCNT hybrid networks, and plasmonic-welded AgNW/SWCNT hybrid networks on a silicon wafer. The AgNW films (Figure 1c) were formed of random networks of AgNWs without significant bundling of wires, and were very uniform over the area of the substrate. However, many AgNWs were connected to the substrate with weak contacts, which led to poor adhesion of the AgNW network to the substrate or to other AgNWs. Thus, the AgNW film has very poor mechanical stability in response to strain. The AgNW/SWCNT hybrid film shown in Figure 1d exhibited SWCNTs uniformly entangled with the AgNWs and bound to the substrate. These SWCNTs, with diameters of several nanometers, help the AgNWs to adhere onto the substrate. Also, the AgNW/SWCNT hybrid structures clearly show that bundles of SWCNTs form electrical branches around the AgNWs and fill the spaces between nanowires. It is notable that the SWCNTs assist in forming good mechanical/electrical connections between AgNWs, and can enhance the mechanical stability of the AgNW/SWCNT hybrid film. In addition, an increased contact area and number of junction points between

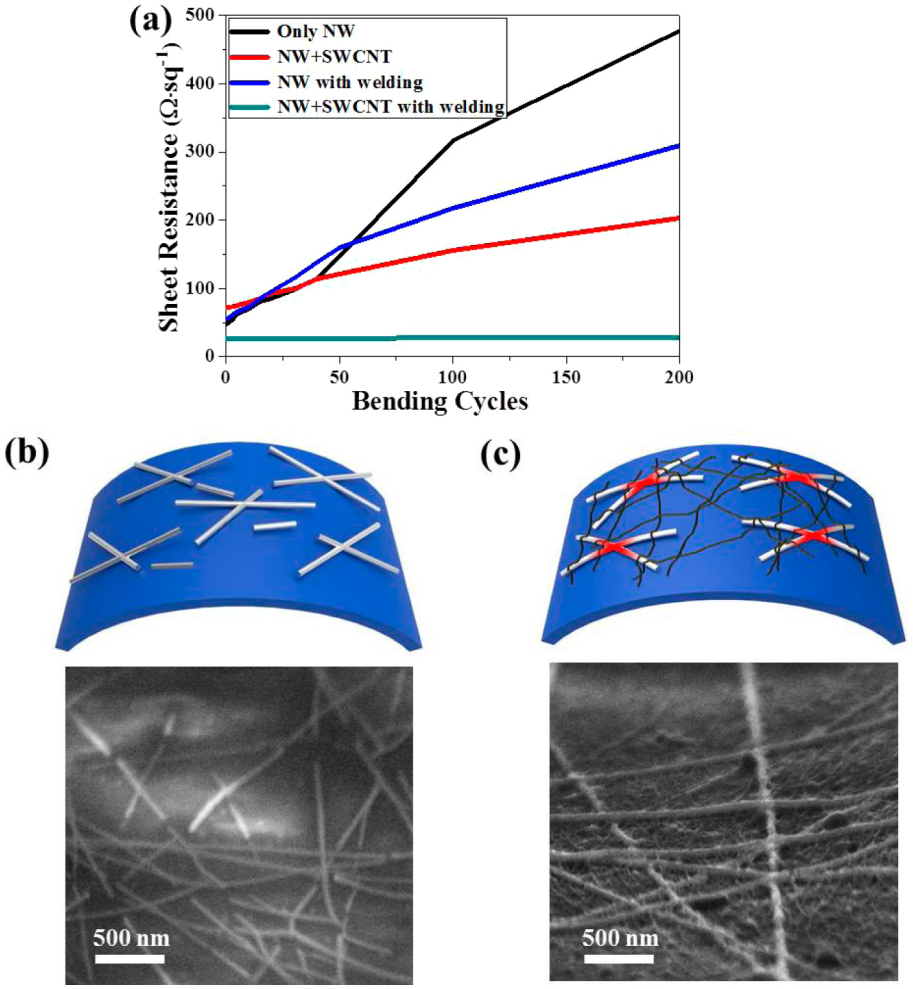

Figure 3. (a) Change in sheet resistance as a function of convex bending cycles for an AgNW electrode, an AgNW/SWCNT hybrid electrode, a plasmon-welded AgNW electrode, and a plasmon-welded AgNW/SWCNT hybrid electrode on PET substrates. Schematics and tilted cross-sectional SEM images of (b) AgNW networks and (c) plasmon-welded AgNW/SWCNT hybrid structures on PET substrate after convex bending test.

AgNWs were achieved using plasmonic welding. The SEM images clearly show melting and fusion of nanowires, leading to improved contact between them, as shown in Figure 1e. Further illumination did not result in a significant change in the resistance of the film, indicating a self-limiting property of the plasmonic welding process (see Figure S2 in the Supporting Information).[33] Figure 1f shows transmission electron microscopy (TEM) images of representative junctions following illumination. The inset is a high-magnification TEM image showing the plasmonic-welded spot between the AgNWs. We observed melting and fusion between the top and bottom AgNWs.

We carried out electrostatic force microscopy (EFM) on the AgNW networks and the AgNW/SWCNT hybrid structures on a PET substrate. In EFM, the electric field gradient near the surface of a sample can be measured using a biased conductive tip.[38] First, a line is scanned to obtain the height profile. Then, a second pass is made over the same line at a controlled height above the surface to map the electric field gradients. The phase shift of the cantilever oscillation shows whether the electrostatic force is attractive or repulsive, as well as the magnitude of the force on the cantilever. We used atomic force microscopy (AFM) and an Au-coated AFM tip. The root-mean-square (RMS) roughness of the AgNW/SWCNT hybrid film was 30 nm (see Figure S3 in the Supporting Information). From the data shown in Figure 2a, the phase shift increased over the AgNW networks due to the attractive force between the AgNWs and the AFM tip. This means that, in an AgNW network film, the electrical connections are confined only to the junctions between the AgNWs, which are prone to degradation during the mechanical bending. However, as shown in Figure 2b, the addition of SWCNTs resulted in an increase in the number of bright regions between the AgNWs, which implies that alternative electrical connections were formed between the AgNWs due to the SWCNTs. This shows that the SWCNT indeed enhanced and stabilized the electrical connections between the AgNWs by forming continuous and dense conduction pathways.

To investigate the electrical conductivity and optical transparency of the AgNW/SWCNT hybrid electrodes, the sheet resistance and transmittance of the films were measured as a function of the SWCNT content, as shown in panels c and d in Figure 2. To obtain high transmittance (over 90%), we prepared samples with 5 μL of AgNW solution, as shown in Figure 2c. As a result, the AgNW electrodes exhibited high sheet resistance and featured defects, which were partially attributed to weak connections between the AgNWs (see Figure S4 in the Supporting Information). However, when the SWCNTs were added, the sheet resistance of the films decreased, which was attributed to the presence of bridging

SWCNTs between adjacent AgNWs, forming a conductive interconnecting material. Furthermore, as the SWCNT content increased, the optical transmittance remained almost unchanged. For 6 μL of AgNW solution (see Figure 2d), the sheet resistance of the AgNW electrodes was significantly lower than that of the AgNW electrodes formed using 5 μL of the AgNW solution. This was attributed to the formation of a three-dimensional conductive network via random percolation. As the SWCNT content was further increased, there was no significant effect on the sheet resistance or transmittance. However, the effect of the SWCNT content on the adhesion between AgNWs and the substrate was very important in obtaining stable and robust AgNW/SWCNT electrodes. One of the most important requirements in flexible TCEs is the stability in response to repeated deformation. To investigate the mechanical stability of the AgNW/SWCNT hybrid electrodes, we measured the sheet resistance as a function of the number of bending cycles for different SWCNT contents, as shown in Figure 2e. The inset shows the setup used to measure the change in the sheet resistance with a bending radius of 5 mm. The sheet resistance increased with the number of bending cycles for all the samples. The resistance of the AgNW electrodes increased rapidly with increasing number of bending cycles, indicating that the inter-NW junctions were unstable and that there was poor mechanical adhesion with the PET substrate. However, the resistance of the AgNW/SWCNT hybrid electrodes was much more stable, and as the CNT content increased further, the sheet resistance decreased because of the enhanced adhesion of the AgNW networks to the substrate or to other AgNWs, consistent with the SEM observations. On the basis of these results, the optimal AgNW content of 6 μL and SWCNT content of 100 μL were used in the hybrid film for the remaining work reported here.

Optical transmittance over a wide wavelength range is an important property for transparent and conductive electrodes.[23] Figure 2f shows the transmission spectra of a SWCNT film, an AgNW film, and an AgNW/SWCNT hybrid film on PET substrate over the visible and infrared spectral region. Because of the low charge carrier density, the SWCNT film showed excellent transparency at wavelengths up to the infrared region. The AgNW film exhibited poor IR transmittance due to the significant increase in reflection caused by the increased skin depth.[39] The transparency of AgNW/SWCNT hybrid films was greater than that of the AgNW film, but less than that of the SWCNT film, regardless of the SWCNT content. The increased optical transmittance of hybrid electrode over IR range is probably due to the change in the surface properties of the AgNW network caused by the covered SWCNTs, leading to decreased reflection. The high transmittance of the conductive film in the range 400−2700 nm is especially important for flexible solar cells because a significant fraction of the power occurs at near-IR wavelengths.[23] The work function is also important for the application of OLEDs and solar cell. The work function of the plasmonic-welded AgNW/SWCNT hybrid film was 5.39 eV, and it is suitable for anode of OLEDs and solar cell due to the relatively high work function.

Figure 3a shows the sheet resistance of several flexible electrodes with different structures on the PET substrates as a function of the number of convex bending cycles. The resistance of the AgNW electrodes following this mechanical stressing was dominated by the contacts between the nanowires and adhesion to the substrate. When the AgNW electrodes were bent, the AgNWs may slide, break, and separate from the substrate. Such problems in the nanowire contacts may lead to a significant increase in the resistance from 53 to 478 Ω sq^{-1}. The plasmon-welded AgNW-only electrodes showed an increase from 61 to 309 Ω sq^{-1}. Following repeated convex bending cycles, the sheet resistance of the AgNW/SWCNT hybrid electrodes increased from 73 to 203 Ω sq^{-1} after bending. This demonstrates that the SWCNTs can significantly improve the resilience to cyclic convex bending. The plasmonic-welded AgNW/SWCNT hybrid electrodes exhibited the lowest initial resistance of 26 Ω sq^{-1}. The superior electrical conductance of these electrodes was attributed to the strong interbundle junctions.[40] Furthermore, the change in resistance in response to 200 convex bending cycles from 26 to 27 Ω sq^{-1} was less than 3.9%. This demonstrates that the synergistic effects of combining the SWCNTs, which are inherently flexible conducting interconnectors, and plasmonic welding to the AgNW networks can be useful for flexible electronics applications. AgNW deposited on PET substrates are very coarse and can be easily detached or broken by mechanical strain due to the weak adhesion to PET substrate, as shown in Figure 3b. Thus, the increase in resistance following repeated convex bending cycles is mainly due to failed electrical contacts between AgNWs. In contrast, the plasmon-welded AgNW/SWCNT hybrid electrodes showed no breaks at junctions between the AgNWs and, following repeated convex bending cycles, a stable morphology was observed that was covered with the SWCNT network, as shown in Figure 3c. It is notable that the SWCNTs assist a tight connection between AgNWs and the substrate, protecting the AgNWs from being damaged and detached under repetitive strain cycles. On the basis of this discussion, SWCNT networks combined with the plasmonic welding process can help to improve the electrical and mechanical stability of AgNW films.

To further investigate the stability of the flexible plasmon-welded AgNW/SWCNT hybrid electrodes, samples were repeatedly bent to convex/concave shapes, as shown in the inset of Figure 4a. We measured the strain-history-dependent resistance, as shown in Figure S5 (see the Supporting Information). This bending strain was repeatedly applied over 200 cycles. Following 200 cycles, the sheet resistance was measured with a flat substrate. As shown in Figure 4a, the sheet resistance of the AgNW electrodes increased considerably from 27 to 531 Ω sq^{-1} after 200 convex/concave bending cycles. For convex bending, the sheet resistance of the film sharply increased with the number of bending cycles. Convex bending induced tensile deformation at the interwire junctions. For concave bending, the sheet resistance increased slowly with the number of bending cycles. Interestingly, the resistance partially recovered when the substrate was relaxed to back to a planar shape. In contrast, the sheet resistance of plasmon-welded AgNW/SWCNT hybrid electrodes remained low, increasing from 26 to only 29 Ω sq^{-1} following 200 convex/concave bending cycles, representing an increase of less than 11.6%. The plasmon-welded AgNW/SWCNT hybrid electrodes exhibited excellent mechanical and electrical stability, even under severe convex/concave cyclic bending. Figure 4b shows optical photographs of an LED integrated circuit connected to the plasmon-welded AgNW/SWCNT hybrid electrodes on a PET substrate in a release state, as well as in concave and convex deformed states. These images show that the brightness of the LED did not change following bending, which implies that our conductors can retain constant resistance with different applied voltages. Figure 4c shows a typical current−voltage (I−V)

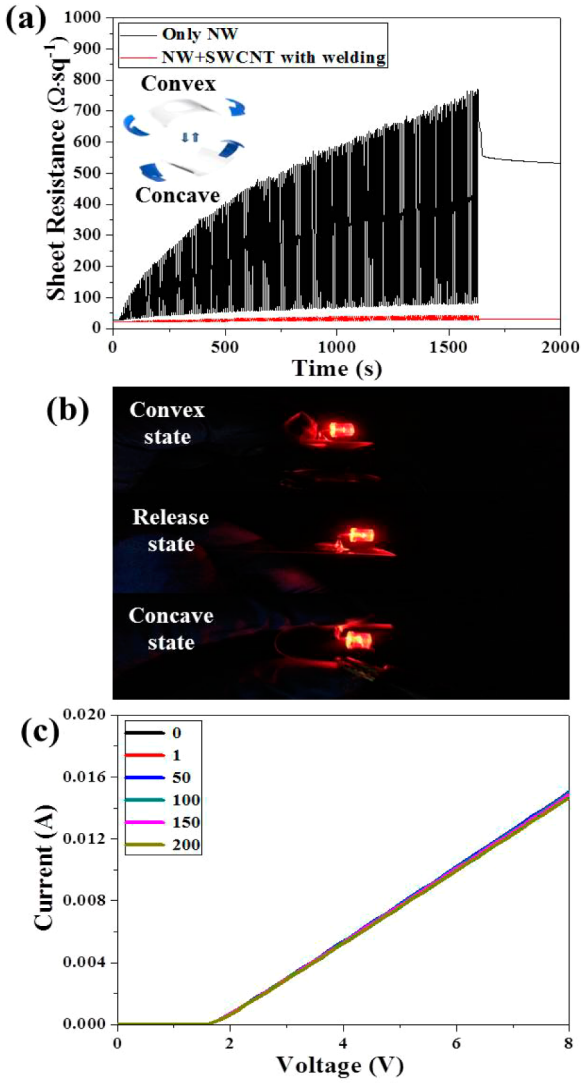

Figure 4. (a) Variations in the sheet resistance as a function of the time in convex/concave cyclic bending for an AgNW electrode and a plasmon-welded AgNW/SWCNT hybrid electrode. The final sheet resistance values were measured after the substrate was relaxed back to release state. Inset shows the schematics of the bending test sample. (b) Optical photographs of the LED integrated circuit connected to the plasmon-welded AgNW/SWCNT hybrid electrode on PET substrate under concave, release, and convex state. (c) Current as a function of voltage curves of the LED circuit with integrated plasmon-welded AgNW/SWCNT hybrid electrodes on PET substrate as a function of the convex bending cycles.

response of the LED circuit with integrated plasmon-welded AgNW/SWCNT hybrid electrodes on a PET substrate as a function of the number convex bending cycles from 0 to 200. Figure S6 in the Supporting Information also shows the *I*−*V* characteristics of the LED circuit under concave bending cycles (see the Supporting Information). In both convex and concave bending cases, there was no significant change in the electrical resistance at different applied voltages, regardless of the number of bending cycles, demonstrating excellent electrical and mechanical stability. Also, the plasmonic-welded AgNW/SWCNT hybrid electrodes exhibited more excellent long-term stability than welded AgNW electrodes under air atmosphere due to the reduce oxidation of the AgNWs by CNTs (see Figure S7 in the Supporting Information). In addition, their optoelectronic properties further improved when they were embedded in a protective layer (see Figure S8 in the Supporting Information).

In summary, we constructed transparent and flexible AgNW/SWCNT hybrid networks on PET substrates along with plasmonic welding. These hybrid networks exhibited highly stable mechanical and electrical properties following repeated deformation. The initial sheet resistance of the hybrid film was 26 Ω sq^{-1}, with >90% optical transmittance over the range 400−2700 nm. After 200 convex bending cycles with a bending radius of 5 mm, the sheet resistance increased to 27 Ω sq^{-1}. Following 200 cycles of convex/concave bending, the resistance changed from 26 to 29 Ω sq^{-1}. This hybrid structure combined with the plasmonic welding process provided excellent stability, low resistance, high transparency over wide wavelength range. Our process and structure are suitable for flexible electronics applications, including touch panels, solar cells, and OLEDs.

■ ASSOCIATED CONTENT

Ⓢ Supporting Information

Experimental section, sheet resistance and transmittance for AgNW with different diameter, tilted cross-sectional SEM images after various illumination time, roughness of the AgNW/SWCNT hybrid film, photographs of AgNW film and AgNW/SWCNT hybrid film, histogram of bending direction with time, *I*−*V* characteristics of the LED circuit, long-term stability under air atmosphere, and optoelectronic properties of plasmon-welded AgNW/SWCNT hybrid electrode with protective layer. This material is available free of charge via the Internet at http://pubs.acs.org.

■ AUTHOR INFORMATION

Corresponding Author

*E-mail: cshan@korea.ac.kr. Tel: +82-2-3290-3354. Fax: +82-2-926-9290.

Author Contributions

‡Authors J.L. and J.Y.W. contributed equally. J.T.K. and B.Y.L. took experiments and analysis. J.Y.W. and C.-S. Han wrote the paper.

Notes

The authors declare no competing financial interest.

■ ACKNOWLEDGMENTS

This work was supported by the Center for Advanced Soft-Electronics funded by the Ministry of Science, ICT and Future Planning as Global Frontier Project (2011-0031635).

■ REFERENCES

(1) Gaynor, W.; Burkhard, G. F.; McGehee, M. D.; Peumans, P. Smooth Nanowire/Polymer Composite Transparent Electrodes. *Adv. Mater.* **2011**, *23*, 2905−2910.

(2) Lee, J.; Lee, P.; Lee, H.; Lee, D.; Lee, S. S.; Ko, S. H.; Very Long, Ag Nanowire Synthesis and Its Application in a Highly Transparent, Conductive and Flexible Metal Electrode Touch Panel. *Nanoscale* **2012**, *4*, 6408−6414.

(3) Lee, M. S.; Lee, K.; Kim, S. Y.; Lee, H.; Park, J.; Choi, K. H.; Kim, H. K.; Kim, D. G.; Lee, D. Y.; Nam, S.; Park, J. U. High-Performance, Transparent, and Stretchable Electrodes Using Graphene−Metal Nanowire Hybrid Structures. *Nano Lett.* **2013**, *13*, 2814−2821.

(4) Coskun, S.; Ates, E. S.; Unalan, H. E. Optimization of Silver Nanowire Networks for Polymer Light Emitting Diode Electrodes. *Nanotechnology* **2013**, *24*, 125202.

(5) Ellmer, K. Past Achievements and Future Challenges in the Development of Optically Transparent Electrodes. *Nat. Photonics* **2012**, *6*, 809−817.
(6) Ge, J.; Yao, H. B.; Wang, X.; Ye, Y. D.; Wang, J. L.; Wu, Z. Y.; Liu, J. W.; Fan, F. J.; Gao, H. L.; Zhang, C. L.; Yu, S. H. Stretchable Conductors Based on Silver Nanowires: Improved Performance through a Binary Network Design. *Angew. Chem.* **2013**, *125*, 1698−1703.
(7) Lee, J.; Lee, P.; Lee, H. B.; Hong, S.; Lee, I.; Yeo, J.; Lee, S. S.; Kim, T. S.; Lee, D.; Ko, S. H. Room-Temperature Nanosoldering of a Very Long Metal Nanowire Network by Conducting-Polymer-Assisted Joining for a Flexible Touch-Panel Application. *Adv. Funct. Mater.* **2013**, *23*, 4171−4176.
(8) Wu, H.; Kong, D.; Ruan, Z.; Hsu, P. C.; Wang, S.; Yu, Z.; Carney, T. J.; Hu, L.; Fan, S.; Cui, Y. A Transparent Electrode Based on a Metal Nanotrough Network. *Nat. Nanotechnol* **2013**, *8*, 421−425.
(9) Hecht, D. S.; Hu, L.; Irvin, G. Emerging Transparent Electrodes Based on Thin Films of Carbon Nanotubes, Graphene, and Metallic Nanostructures. *Adv. Mater.* **2011**, *23*, 1482−1513.
(10) Lee, J.; Lee, I.; Kim, T. S.; Lee, J. Y. Efficient Welding of Silver Nanowire Networks without Post-Processing. *Small* **2013**, *9*, 2887−2894.
(11) Argun, A. A.; Cirpan, A.; Reynolds, J. R. The First Truly All-Polymer Electrochromic Devices. *Adv. Mater.* **2003**, *15*, 1338−1341.
(12) Lipomi, D. J.; Lee, J. A.; Vosgueritchian, M.; Tee, B. C. K.; Bolander, J. A.; Bao, Z. Electronic Properties of Transparent Conductive Films of PEDOT:PSS on Stretchable Substrates. *Chem. Mater.* **2012**, *24*, 373−382.
(13) Yamada, T.; Hayamizu, Y.; Yamamoto, Y.; Yomogida, Y.; Najafabadi, A. I.; Futaba, D. N.; Hata, K. A Stretchable Carbon Nanotube Strain Sensor for Human-Motion Detection. *Nat. Nanotechnol* **2011**, *6*, 296−301.
(14) Yu, W. J.; Lee, S. Y.; Chae, S. H.; Perello, D.; Han, G. H.; Yun, M.; Lee, Y. H. Small Hysteresis Nanocarbon-Based Integrated Circuits on Flexible and Transparent Plastic Substrate. *Nano Lett.* **2011**, *11*, 1344−1350.
(15) Yu, Z.; Niu, X.; Liu, Z.; Pei, Q. Intrinsically Stretchable Polymer Light-Emitting Devices Using Carbon Nanotube-Polymer Composite Electrodes. *Adv. Mater.* **2011**, *23*, 3989−3994.
(16) Kim, K. S.; Zhao, Y.; Jang, H.; Lee, S. Y.; Kim, J. M.; Kim, K. S.; Ahn, J. H.; Kim, P.; Choi, J. Y.; Hong, B. H. Large-Scale Pattern Growth of Graphene Films for Stretchable Transparent Electrodes. *Nature* **2009**, *457*, 706−710.
(17) Wang, Y.; Yang, R.; Shi, Z.; Zhang, L.; Shi, D.; Wang, E.; Zhang, G. Super-Elastic Graphene Ripples for Flexible Strain Sensors. *ACS Nano* **2011**, *5*, 3645−3650.
(18) Lee, S. K.; Kim, B. J.; Jang, H.; Yoon, S. C.; Lee, C.; Hong, B. H.; Rogers, J. A.; Cho, J. H.; Ahn, J. H. Stretchable Graphene Transistors with Printed Dielectrics and Gate Electrodes. *Nano Lett.* **2011**, *11*, 4642−4646.
(19) De, S.; Higgins, T. M.; Lyons, P. E.; Doherty, E. M.; Nirmalraj, P. N.; Blau, W. J.; Boland, J. J.; Coleman, J. N. Silver Nanowire Networks as Flexible, Transparent, Conducting Films: Extremely High DC to Optical Conductivity Ratios. *ACS Nano* **2009**, *3*, 1767−1774.
(20) Yu, Z.; Li, L.; Zhang, Q.; Lu, W.; Pei, Q. Silver Nanowire-Polymer Composite Electrodes for Efficient Polymer Solar Cells. *Adv. Mater.* **2011**, *23*, 4453−4457.
(21) Xu, F.; Zhu, Y. Highly Conductive and Stretchable Silver Nanowire Conductors. *Adv. Mater.* **2012**, *24*, 5117−5122.
(22) Kumar, A.; Zhou, C. The Race To Replace Tin-Doped Indium Oxide: Which Material Will Win? *ACS Nano* **2010**, *4*, 11−14.
(23) Tokuno, T.; Nogi, M.; Jiu, J.; Suganuma, K. Hybrid Transparent Electrodes of Silver Nanowires and Carbon Nanotubes: a Low-Temperature Solution Process. *Nanoscale Res. Lett.* **2012**, *7*, 281−285.
(24) Lee, J. Y.; Connor, S. T.; Cui, Y.; Peumans, P. Solution-Processed Metal Nanowire Mesh Transparent Electrodes. *Nano Lett.* **2008**, *8*, 689−692.
(25) Madaria, A. R.; Kumar, A.; Zhou, C. Large Scale, Highly Conductive and Patterned Transparent Films of Silver Nanowires on Arbitrary Substrates and Their Application in Touch Screens. *Nanotechnology* **2011**, *22*, 245201.
(26) Yu, Z.; Zhang, Q.; Li, L.; Chen, Q.; Niu, X.; Liu, J.; Pei, Q. Highly Flexible Silver Nanowire Electrodes for Shape-Memory Polymer Light-Emitting Diodes. *Adv. Mater.* **2011**, *23*, 664−668.
(27) Lee, P.; Lee, J.; Lee, H.; Yeo, J.; Hong, S.; Nam, K. H.; Lee, D.; Lee, S. S.; Ko, S. H. Highly Stretchable and Highly Conductive Metal Electrode by Very Long Metal Nanowire Percolation Network. *Adv. Mater.* **2012**, *24*, 3326−3332.
(28) Hu, L. B.; Wu, H.; Cui, Y. Metal Nanogrids, Nanowires, and Nanofibers for Transparent Electrodes. *MRS Bull.* **2011**, *36*, 760−765.
(29) Hu, L. B.; Kim, H. S.; Lee, J. Y.; Peumans, P.; Cui, Y. Scalable Coating and Properties of Transparent, Flexible, Silver Nanowire Electrodes. *ACS Nano* **2010**, *4*, 2955−2963.
(30) Tokuno, T.; Nogi, M.; Karakawa, M.; Jiu, J.; Nge, T. T.; Aso, Y.; Suganuma, K. Fabrication of Silver Nanowire Transparent Electrodes at Room Temperature. *Nano Res.* **2011**, *4*, 1215−1222.
(31) Akter, T.; Kim, W. S. Reversibly Stretchable Transparent Conductive Coatings of Spray-Deposited Silver Nanowires. *ACS Appl. Mater. Interfaces* **2012**, *4*, 1855−1859.
(32) Coskun, S.; Ates, E. S.; Unalan, H. E. Optimization of Silver Nanowire Networks for Polymer Light Emitting Diode Electrodes. *Nanotechnology* **2013**, *24*, 125202.
(33) Garnett, E. C.; Cai, W. S.; Cha, J. J.; Mahmood, F.; Connor, S. T.; Christoforo, M. G.; Cui, Y.; McGehee, M. D.; Brongersma, M. L. Self-Limited Plasmonic Welding of Silver Nanowire Junctions. *Nat. Mater.* **2012**, *11*, 241−249.
(34) Zhu, R.; Chung, C. H.; Cha, K. C.; Yang, W.; Zheng, Y. B.; Zhou, H.; Song, T. B.; Chen, C. C.; Weiss, P. S.; Li, G.; Yang, Y. Fused Silver Nanowires with Metal Oxide Nanoparticles and Organic Polymers for Highly Transparent Conductors. *ACS Nano* **2011**, *5*, 9877−9882.
(35) Madaria, A. R.; Kumar, A.; Ishikawa, F. N.; Zhou, C. W. Uniform, Highly Conductive, and Patterned Transparent Films of a Percolating Silver Nanowire Network on Rigid and Flexible Substrates Using a Dry Transfer Technique. *Nano Res.* **2010**, *3*, 564−573.
(36) Tantang, H.; Ong, J. Y.; Loh, C. L.; Dong, X.; Chen, P.; Chen, Y.; Hu, X.; Tan, L. P.; Li, L. J. Using Oxidation to Increase the Electrical Conductivity of Carbon Nanotube Electrodes. *Carbon* **2009**, *47*, 1867−1870.
(37) Halas, N. J.; Lal, S.; Chang, W. S.; Link, S.; Nordlander, P. Plasmons in Strongly Coupled Metallic Nanostructures. *Chem. Rev.* **2011**, *111*, 3913−3961.
(38) Colchero, J.; Gil, A.; Baró, A. M. Resolution Enhancement and Improved Data Interpretation in Electrostatic Force Microscopy. *Phys. Rev. B* **2001**, *64*, 245403.
(39) Hu, L.; Hecht, D. S.; Grüner, G. Infrared Transparent Carbon Nanotube Thin Films. *Appl. Phys. Lett.* **2009**, *94*, 081103.
(40) Ma, W.; Song, L.; Yang, R.; Zhang, T.; Zhao, Y.; Sun, L.; Ren, Y.; Liu, D.; Liu, L.; Shen, J.; Zhang, Z.; Xiang, Y.; Zhou, W.; Xie, S. Directly Synthesized Strong, Highly Conducting, Transparent Single-Walled Carbon Nanotube Films. *Nano Lett.* **2007**, *7*, 2307−2311.